

Self-organized evolution of Ge/Si(001) into intersecting bundles of horizontal nanowires during annealing

J. J. Zhang^{*}, A. Rastelli, O. G. Schmidt, D. Scopece, L. Miglio, and F. Montalenti

Citation: *Appl. Phys. Lett.* **103**, 083109 (2013); doi: 10.1063/1.4818717

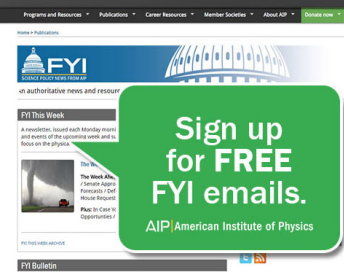
View online: <http://dx.doi.org/10.1063/1.4818717>

View Table of Contents: <http://aip.scitation.org/toc/apl/103/8>

Published by the American Institute of Physics



Fearful for the future of science?



Self-organized evolution of Ge/Si(001) into intersecting bundles of horizontal nanowires during annealing

J. J. Zhang,^{1,a)} A. Rastelli,^{1,2} O. G. Schmidt,¹ D. Scopece,³ L. Miglio,³ and F. Montalenti³

¹*Institute for Integrative Nanosciences, IFW Dresden, D-01069 Dresden, Germany*

²*Institute of Semiconductor and Solid State Physics, University Linz, A-4040 Linz, Austria*

³*L-NESS and Department of Materials Science, University of Milano-Bicocca, I-20125 Milano, Italy*

(Received 17 June 2013; accepted 28 July 2013; published online 20 August 2013)

We report the observation of large scale self-assembly of long horizontal nanowires into orthogonally oriented bundles, during *in situ* annealing of a few monolayers of Ge on Si(001). Results are interpreted in terms of a collective wave-propagation mechanism, previously suggested for interpreting ripple faceting on Ge/Si(1 1 10) surfaces. Quantitative agreement between experiments and theory is found. The onset of the mechanism, the number of wires in the bundles, and their total density can be controlled by carefully tuning the growth parameters. © 2013 AIP Publishing LLC. [<http://dx.doi.org/10.1063/1.4818717>]

Deposition of Ge on Si(001) leads, under rather broad experimental conditions, to Stranski–Krastanow (SK) growth, where three-dimensional (3D) islands form on the top of a thin wetting layer (WL).^{1,2} Careful investigation of Ge/Si(001) allows understanding the key fundamental mechanisms underlying this growth modality, thus facilitating the interpretation of the behavior of more complex systems of broad interest, such as In(Ga)As/GaAs(001). The main driving forces, surface-energy minimization, strain release, and intermixing, are indeed very similar.^{2–5} Besides the purely scientific interest, Ge islands on Si are appealing for potential applications as stressors, which beneficially alter the electronic properties of Si,^{6,7} as phonon scatterers for reducing thermal conductivity⁸ and as single-hole supercurrent transistors.⁹

The demonstration of coherent 3D islands formation following Ge deposition was reported in 1990.^{10,11} In particular, in Ref. 11, clear evidence of “huts” bounded by {105} facets was provided. A justification for such high-index orientation was not straightforward, owed to the expected high-energy surface cost. However, it was later shown that a major reconstruction takes place, leading to a very efficient reduction of the dangling-bond density and virtually eliminating the as-cut staircase configuration.^{12–14} Additional calculations based on Density Functional Theory (DFT) immediately followed, showing that Ge(105) is actually strongly stabilized^{14–16} by the compressive strain determined by the incomplete relaxation of the mismatch. It was clear from the actual surface-energy values that Ge(105), compressed at the Si lattice parameter, could compete in stability with Ge(001)/Si(001).^{5,14–18} More recent results¹⁹ demonstrated that the surface-energy of Ge(105) is even lower than previously reported, resulting in a preferred orientation with respect to (001). A compelling experimental evidence of the tendency towards maximizing {105} exposure was recently reported for Ge growth on a vicinal Si(1 1 10) surface.²⁰

There, a perfectly {105} faceted WL was demonstrated, in the form of a uniform array of horizontal ripples and all oriented in the same direction because of the special (1 1 10) orientation. A collective wave-model was proposed for the onset of such a coherent pattern: starting from an isolated ripple, lateral replication takes place generating close-packed satellites with equal base widths. Despite yielding quantitative agreement with the experiments, the model remained an educated guess, as no direct experimental proof of the “propagating” wave was provided, due to the short time scale involved in the process. Is it possible to observe a similar behavior on a conventional (001) substrate? Before answering this question it is worth noting that ripple faceting on a (1 1 10) surface is easier than on (001) because of thermodynamic (the surface energy of the (1 1 10) substrate is larger¹⁹), geometrical (a ripple bounded by {105} facets can only develop in one direction²⁰), and kinetic (on (1 1 10) the sequence of double steps determines a preferred diffusion direction at the mesoscale²¹) reasons. In addition, the well-known elastic repulsion between nearby islands^{22,23} may prevent clustering of islands.

Recently, we have discovered that on Si(001) very long, isolated (105)-faceted nanowires²⁴ can be obtained by *in situ* annealing of the Ge WL,²⁵ the key driving force being once again the exposure of low-energy {105} surfaces. In this letter, we shall show that, by a suitable choice of growth parameters, bundles of parallel wires form adjacent to the initial seeds. At variance with the Si(1 1 10) case,²⁰ wires can elongate along two orthogonal directions, yielding a peculiar, tunable, mesoscale self-tessellation of the (001) surface.

Samples were grown by solid-source molecular beam epitaxy (MBE) at a base pressure of 5×10^{-11} mbar. We initially deposit 4.4 monolayers (ML) of Ge with a growth rate of 0.04 ML/s at a substrate temperature (T) of 560 °C. Under these conditions, the critical thickness for the formation of usual huts¹¹ is 4.5 ML. After Ge deposition, the temperature is ramped down and kept at different values (ranging from 500 to 550 °C for 12 h annealing) or kept at 520 °C for different time durations (from 1 to 66 h). Figures 1(a)–1(d) show

^{a)}Current address: Centre for Quantum Computation and Communication Technology, School of Physics, University of New South Wales, Sydney, NSW 2052, Australia. E-mail: Jianjun.Zhang@unsw.edu.au

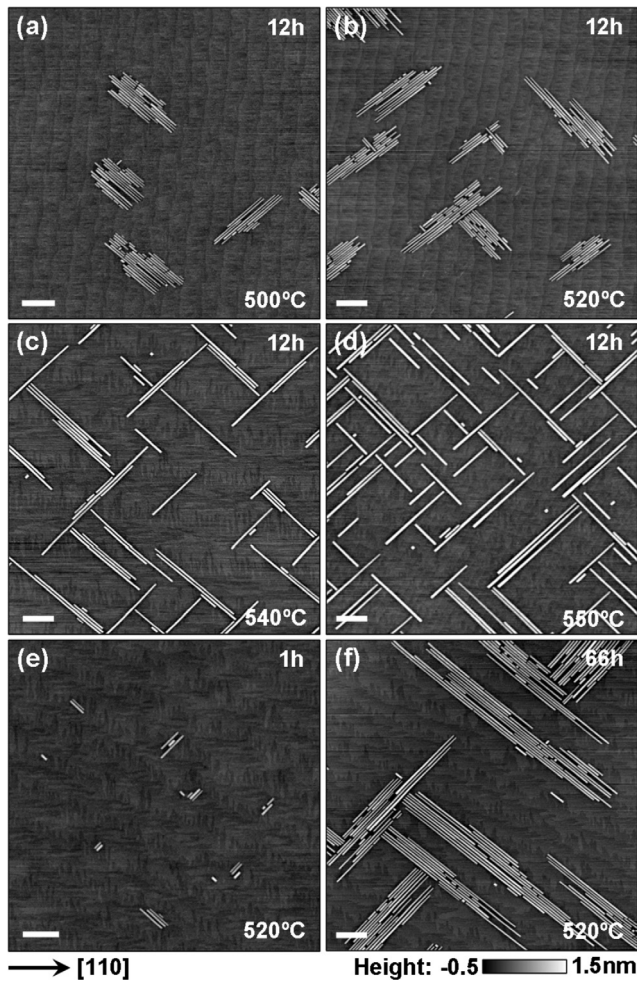


FIG. 1. AFM images showing horizontal Ge nanowire bundles or isolated Ge nanowires on Si(001) substrates obtained after 12 h annealing of a Ge wetting layer at different temperatures: 500 (a), 520 (b), 540 (c), and 550 °C (d), and after 1 h (e), 12 h (b), and 66 h (f) annealing at 520 °C. The Ge wetting layer was obtained by depositing 4.4 ML Ge at a substrate temperature of 560 °C. Scale bar: 250 nm.

atomic force microscopy (AFM) images of Ge nanostructures obtained after 12 h annealing of the 4.4 ML Ge WL at 500, 520, 540, and 550 °C, respectively. At the lower annealing temperatures of 500 and 520 °C, we see “bundles” which consist of tens of closely packed Ge nanowires. They are randomly distributed on the surface and well separated by planar regions consisting of (001) terraces. With increasing annealing T , the number of wires in a bundle tends to decrease and, at 550 °C, wires are almost isolated (similar to the previous observations at 560 °C (Ref. 25)). These observations are quantified in Fig. 2(a), which show the average number of wires per bundle and the density of bundles (or isolated wires) as a function of annealing T . The increase of bundles with increasing annealing T is ascribed to the corresponding increase in nucleation rate.²⁶ If we grow and anneal the sample at the same T of 560 °C, large dislocated islands are formed, quickly gathering material from the wires,²⁷ preventing the observation of the here-above described phenomenology.^{27–29}

Figure 1 indicates that also the size of the nanowires is affected by the substrate temperature during annealing, as quantified in Fig. 2(b). At the lower annealing temperatures

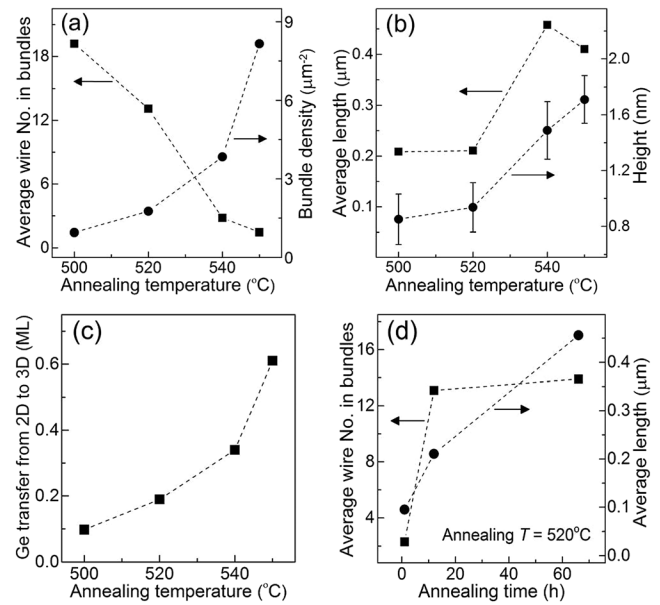


FIG. 2. Average number of wires per bundle ((a), left), surface density of bundles ((a), right), average length of wires ((b), left), wire height ((b), right), and Ge amount transferred from the 2D wetting layer into the 3D nanowires during the 12 h annealing (c), as a function of annealing temperature. Average number of wires per bundle ((d), left) and average length of wires ((d), right) as a function of annealing time at the annealing temperature of 520 °C.

(500 and 520 °C), the bundled wires are about 0.9 nm tall (corresponding to a base width of 9 nm), while at the higher temperatures, the wires have a height of about 1.6 nm [see Fig. 2(b), the error bars indicate the standard deviation]. Also the average wire length tends to increase with T but appears to saturate above 540 °C [see Fig. 2(b)]. We attribute the observed saturation to the increased wire density, which eventually leads to an increased probability of “collisions” (i.e., mutual blocking) between growing wires and also to a decreased amount of Ge material from the WL available for each wire.²⁵ The Ge amount transferred from the WL into the wires (obtained by summing the volume of all wires) increases with increasing annealing T [Fig. 2(c)]. We shall further comment on this observation below.

It is also interesting to investigate the evolution of the nanowire bundles with annealing time. Figures 1(e), 1(b), and 1(f) show AFM images of Ge nanostructures obtained after 1 h, 12 h, and 66 h annealing at 520 °C, respectively. After 1 h annealing, single Ge huts and bundles containing only a few huts are observed. After 12 h annealing, the number of wires in each bundle increases significantly, indicating that new wires nucleate adjacent to the preexisting ones. Simultaneously, the wires grow in length. With further annealing up to 66 h, the wires keep elongating and reach lengths up to a few micrometers. However, no distinct increase of the number of wires per bundle is observed, as seen by comparing Figs. 1(b) and 1(f). These observations are further quantified in Fig. 2(d), showing the average wire number per bundle and average wire length as a function of annealing time.

Let us now supply a theoretical explanation for the rich behavior displayed in Figs. 1 and 2. In Ref. 25, we tackled the energetics of a single, isolated wire, showing how

surface-energy gain prevails over strain relaxation, leading to a preferred wire base width, once the role played by edge energies is considered. Here, instead, we focus our attention on lateral replication of a single wire through the wave-propagation model introduced in Ref. 20 for Ge/Si(1 1 10). There it was shown that once an isolated ripple is created, the system can lower its energy by lateral replication, leading to a set of adjacent ripples of the same size. As for such orientation only two equivalent {105} facets exist,²⁰ all ripples were observed to propagate in the same direction, while in the present case two equivalent elongation/propagation directions, i.e., [100] or [010], are possible, as it is clear from Fig. 1. Furthermore, wave propagation in Ref. 20 was mostly a guess as the surface was quickly covered with {105} ripples and scanning tunneling microscope images only clarified the initial (isolated ripples) and final (full faceting of the surface) configuration. Figs. 1(e), 1(b), and 1(f), instead, capture the progressive evolution. In order to apply the wave model to Ge/Si(001), we modified trivial geometrical factors, re-computed (exploiting a Finite Element Method solver) the elastic energy of the wire + WL + substrate system, and, more importantly, we used Ge/Si(001) surface-energy values instead of Ge/Si(1 1 10), both calculated by *ab initio* methods and reported in Ref. 19.

Here we briefly recall the main ideas entering the calculations. More details are given in the supplementary material.²⁷

Starting from an already existing wire (approximated by a truncated geometry and neglecting the effect of terminations, as in Ref. 25) sitting on a WL, we consider the energy change at fixed volume along the path depicted in Fig. 3(a), where satellite-wires are created, presumably by exploiting the compressive stress field around the wire,² which facilitates removal of atoms around its perimeter.

The energy change during the formation of the first pair of satellites is plotted as a function of the satellite size and for different WL thicknesses (expressed in number N of ML's) in Fig. 3(b), where positive values indicate that propagation should not occur. Below a critical WL thickness, estimated to be around $N = N_c \approx 4.2$ ML, the excavation process raises the energy of the system. This is due to the dependence of surface energies on the WL thickness, producing an increased cost when the distance from the exposed Ge and the outermost Si layer beneath is small.^{5,16,19} Above the critical thickness, instead, the wave propagates

generating satellites with a preferred base size, around ≈ 10 nm in the N-range of interest for the present experiments. As discussed in Ref. 20, such base value characterizes all further satellites originated from the first pair. The results of Fig. 3 allow us to easily interpret the experimental findings. As the initial amount of deposited Ge (4.4 ML) is very close to our predicted critical value, wave propagation should occur only when little material is transferred from the WL to initially isolated (i.e., far apart) wires. Fig. 2(c) tells us that this is the situation at low growth temperatures. At $T = 500^\circ\text{C}$, indeed, the transferred material is of ≈ 0.1 ML only. Notice that this value is obtained after bundles have already formed and partially developed. Therefore the amount of 0.1 ML, although small, overestimates the thinning of the Ge WL at the exact moment where wave propagation starts (the one relevant for the model). After 12 h annealing at $T = 520^\circ\text{C}$ the residual Ge WL approaches the predicted critical thickness. Therefore, further annealing should not promote additional wave propagation, and the only allowed evolution is wire elongation.²⁵ This is nicely confirmed by the experimental data of Figs. 1(b) and 1(f), where the number of wires in each bundle is unchanged, while their lengths keep increasing (Fig. 2(d)). At the highest growth temperature ($T = 550^\circ\text{C}$), instead, there is a ≈ 0.6 ML transfer. This means that the residual WL is, on average, only ≈ 3.8 ML thick. As it is clear from Fig. 3(b), the wave should not develop under this thin-WL condition, and this is the actual situation seen in the experiments (mostly isolated wires). One may still ask why the wave did not form at earlier stages of the annealing, when the WL thickness was still sufficiently large. We speculate that at high enough T , as soon as the wave process is attempted, e.g., by expelling adatoms at the long sides of the wire, highly mobile adatoms quickly diffuse away (some of them eventually incorporating at the short sides), without leading to actual nucleation of a new satellite wire. As the process proceeds, the WL becomes thinner so that lateral replication eventually becomes unfavorable. Finally, we derive from Fig. 2(c) that the residual thickness at $T = 540^\circ\text{C}$ is only slightly smaller than the theoretical limiting value. Indeed, Fig. 1(c) shows only “attempts” of lateral replication, i.e., bundles consist of up to at most 3–5 wires, confirming the proximity to the critical condition.

The agreement with the experiments is not limited to predicting critical thicknesses. From Fig. 3(b) we see that the predicted lateral size of the wires is of the order of 10 nm

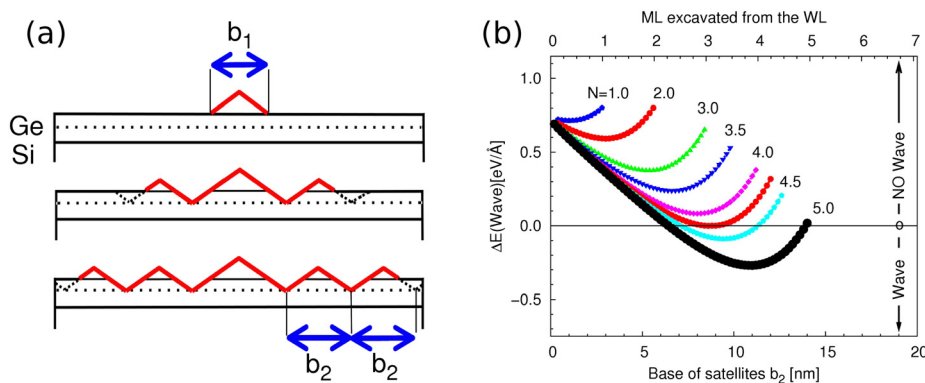


FIG. 3. (a) 2D sketch of the creation of a wave starting from a single precursor of base b_1 lying on a N -ML-thick wetting layer. (b) Difference in total energy between an isolated wire and a wire with two satellites of variable base. In (b) the red curve tangent to the zero value is the one obtained for $N = N_c = 4.25$ ML. In the actual calculations the base of the initial wire was set to $b_1 = 10$ nm. The satellites' base b_2 , however, is practically independent of b_1 .²⁰

(1 nm in height), in agreement with the two lowest- T data of Fig. 2(b), i.e., the ones referring to cases where the wave does propagate. Very importantly, this value is some 40% smaller with respect to the typical base size predicted for an isolated wire (determined by a different energetic balance, exploiting however the very same set of microscopic parameters²⁵). This is again in agreement with the results of Fig. 2(b), where the higher- T point corresponds to a situation approaching non-bundled wires (see Figs. 1(c) and 1(d) and Ref. 25).

A full quantitative description (and prediction) of the whole set of results displayed in Fig. 2 would clearly require a more advanced model (e.g., an extension of the approach proposed in Ref. 29), able to estimate to which extent kinetic constraints would frustrate the thermodynamic limit implicitly assumed in our calculations, and tackling a subtle issue such as determining critical sizes for nucleation of stable “seeds,” eventually leading to formation of mature wires or pyramids.^{30,31} In addition, some limited Si-Ge intermixing taking place during annealing^{25,27} would need to be considered. However, some further qualitative conclusions can be reached. For instance, at the low annealing temperatures it is clear from Figs. 1(e), 1(b), and 1(f) that elongation and wave-replication proceed on similar time scales in the initial stages, both being frustrated by the limited mobility and the limited possibility to generate adatoms from the WL (but also nucleation barriers at the {105} facets could play an important role at such low temperatures^{29,32}). As the temperature increases, wires easily elongate (reaching the micron scale) as a result of fast mobility. Therefore, the WL quickly gets thinner so that, as above discussed, thermodynamics hinders wave propagation. However, the actual situation is more complex, as mutual-blocking between wires elongating in orthogonal directions starts setting in, leading to a frustration of the elongation, as seen in Fig. 2(b) for the highest annealing T .

In summary, we have shown that deposition of a few ML of Ge on Si(001), followed by *in situ* annealing at a temperature lower than the growth temperature, leads to a remarkable phenomenon. Bundles of nanowires with lengths approaching the micron scale are created during annealing at low temperatures and lead to a mesoscale self-structuring of the surface. Experiments were interpreted by exploiting a wave-propagation model which was previously suggested for explaining the {105} faceting of Si(1 1 10).²⁰ We have shown that the model helps also in explaining how lateral replication can be controlled by temperature. The quantitative agreement between experiments and theory confirms the validation of the model. Collective models for huts nucleation were already reported in the literature, in the case of SiGe-alloy deposition on Si(001),³³ where it was first suggested that a sequential process was likely to be involved. However, the treatment followed the popular description of SK-growth in terms of surface cost vs. strain release. Instead, here and in some previous papers involving the present theoretical team,^{5,20,25} we are pointing out that creating {105} facets actually lowers the total surface cost, the effect, for these low aspect-ratio structures, being much stronger than strain-release. Semiconductor heteroepitaxial systems show striking similarities. InAs huts have also been observed

on InGaAs/InP substrate.^{34,35} We anticipate that the phenomena of forming nanowires or nanowire bundles via the reduction of surface energy should appear in three-five material systems, too.

We acknowledge the financial support by the DFG SPP1386 and the EU (Project No. 263440), G. Katsaros for stimulating this work, S. Kiravittaya and J. Tersoff for discussions, and P. Chen and D. J. Thurmer for MBE assistance.

- ¹J. Stangl, V. Holy, and G. Bauer, *Rev. Mod. Phys.* **76**, 725 (2004).
- ²L. Miglio and F. Montalenti, *Silicon-Germanium (SiGe) Nanostructures: Production, Properties and Applications in Electronics*, edited by Y. Shiraki and N. Usami (Woodhead Publishing Limited, Cambridge, 2011).
- ³L. G. Wang, P. Kratzer, M. Scheffler, and N. Moll, *Phys. Rev. Lett.* **82**, 4042 (1999).
- ⁴G. Costantini, A. Rastelli, C. Manzano, P. Acosta-Diaz, G. Katsaros, R. Songmuang, O. G. Schmidt, H. v. Känel, and K. Kern, *J. Cryst. Growth* **278**, 38 (2005).
- ⁵M. Brehm, F. Montalenti, M. Grydlik, G. Vastola, H. Lichtenberger, N. Hrauda, M. J. Beck, T. Fromherz, F. Schäffler, L. Miglio, and G. Bauer, *Phys. Rev. B* **80**, 205321 (2009).
- ⁶O. G. Schmidt and K. Eberl, *IEEE Trans. Electron Devices* **48**, 1175 (2001).
- ⁷V. Jovanović, C. Biasotto, L. K. Nanver, J. Moers, D. Grützmacher, J. Gerharz, G. Mussler, J. van der Cingel, J. J. Zhang, G. Bauer, O. G. Schmidt, and L. Miglio, *IEEE Electron Device Lett.* **31**, 1083 (2010).
- ⁸G. Pernot, M. Stoffel, I. Savic, F. Pezzoli, P. Chen, G. Savelli, A. Jacquot, J. Schumann, U. Denker, I. Mönch, Ch. Deneke, O. G. Schmidt, J. M. Rampnoux, S. Wang, M. Plissonnier, A. Rastelli, S. Dilhaire, and N. Mingo, *Nature Mater.* **9**, 491 (2010).
- ⁹G. Katsaros, P. Spathis, M. Stoffel, F. Fournel, M. Mongillo, V. Bouchiat, F. Lefloch, A. Rastelli, O. G. Schmidt, and S. De Franceschi, *Nat. Nanotechnol.* **5**, 458 (2010).
- ¹⁰D. Eaglesham and M. Cerullo, *Phys. Rev. Lett.* **64**, 1943 (1990).
- ¹¹Y.-W. Mo, D. E. Savage, B. S. Swartzentruber, and M. G. Lagally, *Phys. Rev. Lett.* **65**, 1020 (1990).
- ¹²P. Raiteri, D. B. Migas, L. Miglio, A. Rastelli, and H. von Känel, *Phys. Rev. Lett.* **88**, 256103 (2002).
- ¹³Y. Fujikawa, K. Akiyama, T. Nagao, T. Sakurai, M. G. Lagally, T. Hashimoto, Y. Morikawa, and K. Terakura, *Phys. Rev. Lett.* **88**, 176101 (2002).
- ¹⁴D. B. Migas, S. Cereda, F. Montalenti, and L. Miglio, *Surf. Sci.* **556**, 121 (2004).
- ¹⁵G. H. Lu, M. Cuma, and F. Liu, *Phys. Rev. B* **72**, 125415 (2005).
- ¹⁶G. H. Lu and F. Liu, *Phys. Rev. Lett.* **94**, 176103 (2005).
- ¹⁷O. E. Shklyav, M. J. Beck, M. Asta, M. J. Miksis, and P. W. Voorhees, *Phys. Rev. Lett.* **94**, 176102 (2005).
- ¹⁸B. J. Spencer and J. Tersoff, *Appl. Phys. Lett.* **96**, 073114 (2010).
- ¹⁹D. Scopece, F. Montalenti, and M. J. Beck, *Phys. Rev. B* **85**, 085312 (2012).
- ²⁰G. Chen, B. Sanduijav, D. Matei, G. Springholz, D. Scopece, M. J. Beck, F. Montalenti, and L. Miglio, *Phys. Rev. Lett.* **108**, 055503 (2012).
- ²¹P. D. Skutnick, A. Sgarlata, A. Balzarotti, N. Motta, A. Ronda, and I. Berbezier, *Phys. Rev. B* **75**, 033305 (2007).
- ²²H. T. Johnson and L. B. Freund, *J. Appl. Phys.* **81**, 6081 (1997).
- ²³J. Floro, G. A. Lucadamo, E. Chason, L. B. Freund, M. Sinclair, R. D. Twetten, and R. Q. Hwang, *Phys. Rev. Lett.* **80**, 4717 (1998).
- ²⁴The “nanowires” discussed here and in Ref. 25 are identical to the usual “huts” (Ref. 11) in terms of exposed facets. The nomenclature is based on the length. “Huts” have a typical length of tens of nanometers, while “nanowires” are usually a few hundred nanometers or even a few micrometers. On Si(1 1 10), instead, only two equivalent {105} facets are available, and the whole surface is completely faceted, and this justifies per se a different name, “ripples” (Ref. 20).
- ²⁵J. J. Zhang, G. Katsaros, F. Montalenti, D. Scopece, R. O. Rezaev, C. Mickel, B. Rellinghaus, L. Miglio, S. De Franceschi, A. Rastelli, and O. G. Schmidt, *Phys. Rev. Lett.* **109**, 085502 (2012).
- ²⁶J. Tersoff and F. K. LeGoues, *Phys. Rev. Lett.* **72**, 3570 (1994).

- ²⁷See supplementary material at <http://dx.doi.org/10.1063/1.4818717> for the large dislocated islands and wet chemical etching results and a detailed theoretical calculation.
- ²⁸M. R. McKay, J. Shumway, and J. Drucker, *J. Appl. Phys.* **99**, 094305 (2006).
- ²⁹M. R. McKay, J. A. Venables, and J. Drucker, *Phys. Rev. Lett.* **101**, 216104 (2008).
- ³⁰I. Goldfarb, P. T. Hayden, J. H. G. Owen, and G. A. D. Briggs, *Phys. Rev. B* **56**, 10459 (1997).
- ³¹L. V. Arapkina and V. A. Yuryev, *Phys. Rev. B* **82**, 045315 (2010).
- ³²D. E. Jesson, G. Chen, K. M. Chen, and S. J. Pennycook, *Phys. Rev. Lett.* **80**, 5156 (1998).
- ³³D. E. Jesson, K. M. Chen, S. J. Pennycook, T. Thundat, and R. J. Warmack, *Phys. Rev. Lett.* **77**, 1330 (1996).
- ³⁴H. Hwang, S. Yoon, H. Kwon, E. Yoon, H. S. Kim, J. Y. Lee, and B. Cho, *Appl. Phys. Lett.* **85**, 6383 (2004).
- ³⁵P. Kratzer, A. Chakrabarti, Q. K. K. Liu, and M. Scheffler, *New J. Phys.* **11**, 073018 (2009).